RESEARCH ARTICLE

METAGENOMICS COMBINED WITH HIGH-THROUGHPUT SEQUENCING REVEALS THE METHANOGENIC POTENTIAL OF FRESH CORN STRAW UNDER THERMOPHILIC AND HIGH OLR

Jinzhi HUANG*[1], Xiaoting YAN*[2], Zhen LIU[1], Mengyi WANG[1], Yangyang HU[3], Zhenyu LI[3], Minsong LIN (✉)[4], Yiqing YAO (✉)[1,5]

1 College of Mechanical and Electronic Engineering, Northwest A&F University, Yangling 712100, China.
2 School of Ecology and Environment, Northwestern Polytechnical University, Xi'an 710072, China.
3 College of Food Science and Engineering, Northwest A&F University, Yangling 712100, China.
4 Chinese Academy for Environmental Planning, Ministry of Ecology and Environment of the People's Republic of China, Beijing 100012, China.
5 Northwest Research Center of Rural Renewable Energy, Exploitation and Utilization of Ministry of Agriculture, Northwest A&F University, Yangling 712100, China.

*These authors contribute equally to the work

HIGHLIGHTS

- Methane production from fresh straw was 7.50% higher than dry straw.
- The structure of fresh straw was more conducive to be degraded.
- Organic components of fresh straw was richer and higher than dry straw.
- *Clostridium_sensu_stricto_1*, *Sporosarcina* and *Methanosarcinia* dominated AD.
- Metagenomics revealed *Metanosarcinia* adapted to high VFA stress via multiple pathways.

GRAPHICAL ABSTRACT
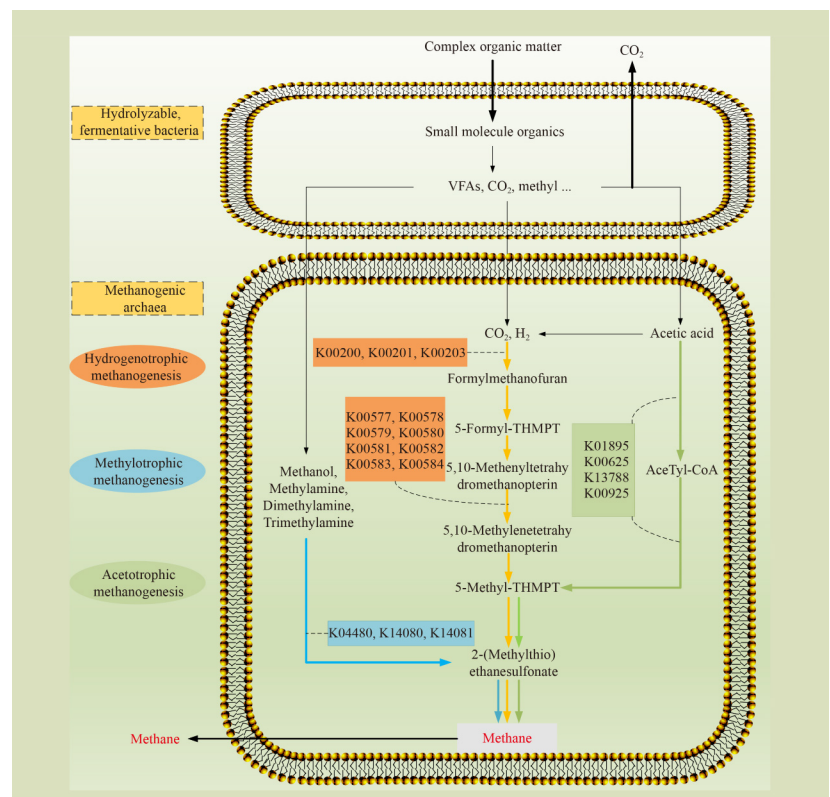
ABSTRACT

Dry corn straw (DCS) is usually used in anaerobic digestion (AD), but fresh corn straw (FCS) has been given less consideration. In this study, the thermophilic AD of single-substrate (FCS and DCS) and co-digestion (straw with cattle manure) were investigated. The results show that when FCS was used as the single-substrate for AD, the methane production was 144 mL·g^{-1}·VS^{-1}, which was 7.5% and 19.6% higher than that of single DCS and FCS with cattle manure, respectively. In addition, the structure of FCS was loose and coarse, which was easier to be degraded than DCS. At the hydrolysis and acidification stages, *Clostridium_sensu_stricto_1*, *Clostridium_sensu_stricto_7* and *Sporosarcina* promoted the decomposition of organic matter, leading to volatile fatty acids (VFAs) accumulation. *Methanosarcina* (54.4%) activated multifunctional methanogenic pathways to avoid the VFAs inhibition, which was important at the CH$_4$ production stage. The main pathway was hydrogenotrophic methanogenesis, with genes encoding formylmethanofuran dehydrogenase (K00200-K00203) and tetrahydromethanopterin S-methyltransferase (K00577-K00584). *Methanosarcina* also activated acetotrophic and methylotrophic methanogenesis pathways, with genes encoding acetyl phosphate (K13788) and methyl-coenzyme M reductase (K04480, K14080 and K14081), respectively. In the co-digestion, the methanogenic potential of FCS was also confirmed. This provides a scientific basis for regulating AD of crop straw.

1   INTRODUCTION

The world is facing multiple pressures, such as environmental pollution and energy shortages, which forces countries to look for new technologies to generate renewable energy and reduce their dependence on current energy sources such as coal, gasoline and syngas[1,2]. In this context, renewable energy is favored over the world because of its clean, pollution-free and renewable advantages. Among the various renewable energy sources, biomass resources account for about 60%[3].

There are many types of biomass raw materials, including crop residues (such as straw), forestry waste and municipal solid waste[4]. Crop residues have recently received large attention as a potentially considerable source of renewable energy. On a global scale, 3.8×10^9 Mg·yr^{-1} of crop residues, with 11×10^{15} kcal, are estimated to be available, of which approximately three fourths are made up of straw residues[5]. Unfortunately, a large proportion of the straw residues is directly burned in the field, which not only causes serious environmental pollution, but also wastes biomass resources[6]. However, crop straw have high energy density that can be usually be used for CH$_4$ production via AD[7].

Due to the high carbon concentration of straw, crop straw cannot provide a balanced C:N ratio for AD microorganisms[8]. Also, straw is composed of cellulose, hemicellulose and lignin, the structure is cross-linked and complex, which is difficult to be effectively degraded by microorganisms. Both of which lead to low AD efficiency.

Given this imbalance C:N, the main technology used is anaerobic co-digestion and there have been many successful examples[9,10]. Studies have shown that co-digestion establishes a positive synergy in balancing the C:N ratio and system buffering capacity, and also provides missing nutrients to effectively perform the AD process and ultimately increase CH$_4$ production[11]. Additionally, using fresh straw instead of dry straw for AD can solve the problem of its refractory degradation. In fact, fresh straw is more easily degraded because of its porous surface structure[12]. Also, fresh straw maintains the original nutritional properties, which has good carbon retention capacity during storage and allows longer storage time than dry straw. The organic compounds are more abundant and higher than dry straw. These characteristics help to improve the degradation ratio and methanogenic efficiency of straw[13]. Large amounts of harvest corn straw is becoming

dry and discarded in the field, which results in a large loss of carbohydrates and soluble components during the drying process. DCS is generally associated with lower biogas production[14]. Therefore, it is of great significance to study an efficient, stable and safe method to convert corn straw into renewable energy. The most important aspect of the research is the mechanisms behind the efficient dry matter preservation and material conversion of fresh and dry straw types, as well as their methane-producing potential and related energy conversion mechanisms also require in-depth exploration and comprehensive evaluation. In this study, FCS and DCS were used as substrates of high solid anaerobic digestion (HS-AD), the methanogenic potential, structural characteristics, intermediate metabolites and microbial metabolism were investigated and compared. To maximize the CH_4 production potential of these two straws, a co-digestion of straw and cattle manure was further performed to balance the digestive system nutrition. The goal was to develop a system for scientifically and rationally using crop straw for energy conversion.

2   MATERIALS AND METHODS

2.1   Sources of corn straw and inoculum

The whole-plant corn straw samples were prepared at the Yangling, Shaanxi Province, China. Corn (cv. Wan Nuo 2000) was harvested in the green (fresh) status. The corn straw was processed into about 1 mm and stored at –20 °C. Some straw was dried at 105 °C for constant weight and stored as DCS. Cattle manure was collected from a cattle farm in Yangling. Effluent from a laboratory AD reactor running at medium temperature (55 ± 1 °C) was used as inoculum.

2.2   Experimental design

The batch experiment was conducted at thermophilic temperature (55 °C) in order to improve degradation ratio of the substrate and thereby the energy conversion efficiency[15].

The reactor total volume was 500 mL and working volume 350 mL. The total solids (TS) concentration was 12%. Each group of experiments was repeated in three times. As different methane production ratios are generated from various materials and conditions[16–18], an experiment on the optimal ratio of cattle manure to corn straw was conducted. Finally, a corn straw to cattle manure ratio of 1:1 was determined as the optimal mixture in this study[19]. The tested combinations are shown in Table 1.

2.3   Analysis method

2.3.1   Methanogenic potential analysis

TS and VS were determined by using standard methods[20]. The crude protein concentration was estimated by multiplying the Kjeldahl nitrogen concentration by 6.25. Total kjeldahl nitrogen (TKN) was determined by using standard methods[20]. The elemental compositions, including C, H, N and O, were tested by an elemental analyzer. The cellulose concentration was determined by ANKOM 200i automatic cellulose analyzer. The amount of biogas production was measured by the drainage method every 24 h. The biogas composition was analyzed using a gas chromatograph equipped with a thermal conductivity detector. The parameters were: inlet 100 °C, detector 150 °C and air flow 30 mL·min⁻¹[21]. The pH was measured with a digital pH meter. VFAs C2–C5 concentration was measured by gas chromatograph equipped with an AE-FFAP column (30 m × 0.25 μm × 0.33 μm), FID detector and total VFAs was calculated as the sum. Excitation emission matrix (EEM) fluorescence spectroscopy was used to characterize the variations of the HS-AD liquid, and the EEM spectroscopy was obtained by measuring the emission (Em) spectra from 200 to 500 nm at 5 nm increments by varying the excitation (Ex) wavelength from 250 to 500 nm at 5 nm increments. Total ammonia nitrogen (TAN) concentration was tested according to the standard method[22]. The concentration of free ammonia nitrogen (FAN) were calculated as[23]:

Table 1   Tested inoculum and substrate ratios

Treatment group	Inoculum:substrate ratio (VS basis)	Substrate	Corn straw:cattle manure ratio (dry weight)
T1	1:4	FCS	1:0
T2	1:4	DCS	1:0
T3	1:4	FCS	1:1
T4	1:4	DCS	1:1

Note: VS, volatile solid.

$$FAN = \frac{TAN}{1 + \frac{10^{-pH}}{K_\alpha}} \qquad (1)$$

where, TAN is total ammonia nitrogen, K_α is a dissociation constant, which reflects on temperature, equals is 3.91×10^{-9} for 55 °C and pH is equal to the pH of the reactor contents.

2.3.2   Structure analysis

Micrographs were obtained by scanning the apparent morphology of corn straw with a scanning electron microscope (SEM; S-4800 High Resolution Scanning Electron Microscope, Hitachi, Tokyo, Japan). Fourier transform infrared spectroscopy (FTIR) spectra of corn straw samples were obtained by using PerkinElmer, FTIR Spectrum GX (Waltham, MA, USA). The corn straw (10 mg) was thoroughly mixed with 200 mg of KBr and the mixture was compressed for preparation of pellets. Each spectrum was the average of 32, coaddition of scans with a total scan time15 s in the IR range of 400–4000 cm^{-1}. The analysis of mechanical properties was completed by using a computer-controlled electronic universal testing machine (UTM6503, Suns, Shenzhen, Guangzhou, China). The outer layer of corn straw (mainly leaves without veins) was divided into rectangular sample strips, and the thickness and width of the outer layer measured with vernier calipers. For each group of five tensile tests, the average was taken as the test value.

2.3.3   DNA extraction and high-throughput sequencing

Microbial samples were collected on 10 and 28 days (stable and end phases, respectively) after commencing AD, and were marked as S_T1 (samples of single-substrate FCS system in stable phase) and S_T2 (samples of single-substrate DCS system in stable phase), S_T3 (samples of co-digested FCS system in stable phase), S_T4 (samples of co-digested DCS system in stable phase), E_T1 (samples of end single-substrate FCS system), E_T2 (samples of end single-substrate DCS system), E_T3 (samples of end co-digestion FCS system) and E_T4 (samples of end co-digestion DCS system). Before extracting DNA, the digested sample was centrifuged at 8000 r·min^{-1} for 5 min to separate the sediment layer. This sediment was then frozen at −80 °C for 24 h, and then freeze-dried using a vacuum freeze dryer. The high-throughput 16S rRNA gene amplicon sequencing method was used to describe and characterize the microbial community composition in the biogas slurry. For bacteria, the extracted genomic DNA was amplified with primer 338F (5'-ACTCCTACGGGAGGAGG-CAGCA-3') and reverse primer 806R (5'-GGAC-TACHVGGGTWTCTAAT-3'). PCR amplification was performed in the V4-V5 region of the 16S rRNA gene.

The archaeal were amplified using 524F10extF (5'-TGYCAGCCGCCGCGGTAA-3') and Arch958RmodR (5'-YCCGGCGTTGAVTCCAATT-3') primer pair. The QIIME platform removed low-quality sequences in the original data and distinguishes sequences from different samples based on the tag sequence. Then the optimized sequences were clustered into operational taxonomic units (OTUs) using UPARSE 7.1 with 97% sequence similarity level. The most abundant sequence for each OTU was selected as a representative sequence. To minimize the effects of sequencing depth on alpha and beta diversity measure, the number of 16S rRNA gene sequences from each sample were rarefied to 26,434, which still yielded an average Good's coverage of 99.99%, respectively. The taxonomy of each OTU representative sequence was analyzed by RDP Classifier version 2.2 against the 16S rRNA gene database (e.g., Silva v138) using confidence threshold of 0.7. The community composition of each sample was counted at different species classification levels. Based on the OTUs information, alpha diversity indices including observed OTUs, Chao1 richness, Shannon index and Good's coverage were calculated with Mothur v1.30.1.

2.3.4   Metagenomics analysis

The sequences of non-redundant gene sets were compared with the KEGG gene database (Kyoto Encyclopedia of Genes and Genomes)[24]. This test produced a large data set of metagenomic DNA, with a total of 25.9×10^6 two times 250 bp paired-end sequences. After quality filtering of the sample, 10.1 G and 6.27 G nucleotide bases were retained, respectively. The sum of gene abundance corresponding to KO, Pathway, EC and Module was conducted to calculate the abundance of this functional category. The structure and composition of species, functions or genes in different groups (or samples) was displayed in plots based on the corresponding taxonomic data tables.

2.3.5   Data analysis

Data processing and statistical analyses were performed using Microsoft Excel 2010, IBM SPSS Statistics 24 and Origin 2018. The microbial data and Metagenomics analysis were analyzed on the free online platform of Majorbio cloud platform[25]. The correlation network reflected the correlation of each species at the genus level under a certain environmental condition. A Spearman's correlation between two genera was considered statistically robust if the Spearman's correlation coefficient (ρ) was > 0.5 and the *P*-value was < 0.05. The correlation network and function prediction of the microbial community were performed using the OmicStudio tools.

3 RESULTS AND DISCUSSION

3.1 Gas production

The biogas production is shown in Fig. 1. The time to peak of daily CH_4 production among the four systems differed (Fig. 1(a)). On day 8, the T2 and T4 groups first reached the maximum production, and the CH_4 concentrations were 43.8% and 36.3%, respectively. The T1 and T3 groups reached their peak on day 12, and the concentration of CH_4 were 48.3% and 41.3% respectively. The peak of the FCS system was delayed by 4 days compared with the DCS system, which was due to the conversion ratio of intermediate metabolites. The detailed explanation is presented in Section 3.3.1.

In the single-substrate AD group, the CH_4 content in T1 was greater than that in T2 (Fig. 1(b)), which were 48.3% and 43.8%, respectively. T1 had cumulative CH_4 production at 144 mL·g^{-1} per VS, which was 7.50% higher than T2 (134 mL·g^{-1} per VS) ($P < 0.05$) (Fig. 1(c)). It shows that the FCS system has a higher CH_4 production ratio and cumulative CH_4 production. This was closely related to the characteristics of the raw materials themselves. In Table 2, the VS of FCS was

86.4% ± 1.11%, which was higher than that of DCS (85.3% ± 0.48%), indicating that FCS could retain the concentration of organic compound to a greater extent. This can be verified from the concentration of cellulose, hemicellulose and lignin. The cellulose concentration of FCS (37.5% of TS), the hemicellulose concentration (31.2% of TS) and the crude protein concentration (19.6% of TS) were all higher than those of DCS (34.6% of TS, 26.3% of TS, 12.4% of TS) respectively. The cellulose and hemicellulose degradation ratio of the T1 and T3 groups were higher than those of the T2 and T4 groups (Table 3). Specifically, the cellulose degradation ratio of T1 was 30.0%, which was higher than that of T2 (29.8%). The cellulose degradation ratio of T3 was 36.4%, which was higher than that of T4 (34.6%). The hemicellulose degradation ratio of T1 was 27.0%, which was higher than that of T2 (23.6%). The hemicellulose degradation ratio of T3 was 16.5%, which was higher than that of T4 (15.7%). This is due to the higher organic compound concentration in FCS provided the sufficient source of nutrients for the metabolism of microorganisms. The degradation ratio of cellulose and hemicellulose in the FCS system would increase. Therefore, the methane production of the FCS system was high. In the co-digestion group, T3 and T4 had the same characteristics as the
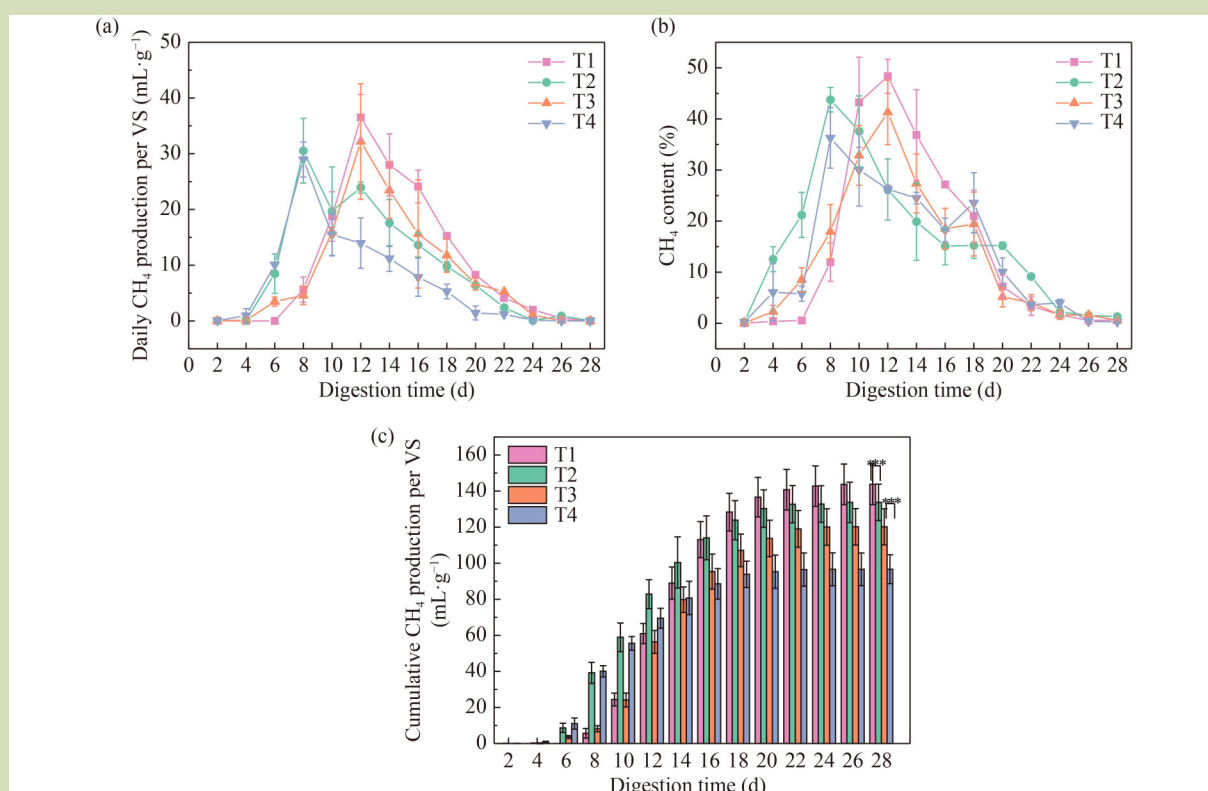

Fig. 1 Variation of gas production with time. (a) Daily CH_4 production; (b) CH_4 concentration; (c) cumulative CH_4 production.

Table 2   Basic physicochemical properties of test materials

Parameter	FCS	DCS	Cattle manure	Inoculum
TS (%)	94.0 ± 0.40	–	20.1 ± 0.46	7.1 ± 0.02
VS (%)	86.4 ± 1.11	85.3 ± 0.48	16.9 ± 0.47	5.3 ± 0.08
C (% of TS)	38.3 ± 7.73	38.0 ± 5.90	34.3 ± 5.26	34.9 ± 5.41
N (% of TS)	2.3 ± 0.71	1.8 ± 0.26	1.7 ± 0.23	2.1 ± 0.72
C:N	17.0 ± 1.52	20.9 ± 1.34	20.7 ± 1.16	16.6 ± 2.30
Cellulose (% of TS)	37.5 ± 1.52	34.6 ± 0.21	34.0 ± 3.96	24.7 ± 0.98
Hemicellulose (% of TS)	31.2 ± 1.67	26.3 ± 0.51	24.2 ± 2.19	21.5 ± 1.23
Lignin (% of TS)	16.9 ± 0.22	19.0 ± 0.32	2.8 ± 0.71	5.4 ± 1.92
Crude protein (% of TS)	19.6 ± 0.37	12.4 ± 0.15	14.1 ± 0.26	13.9 ± 0.30
Elasticity modulus (MPa)	1.7 ± 0.60	5.8 ± 1.81	–	–

Table 3   Utilization ratio of components of digestion substrate

Sample	Cellulose degradation ratio (%)	Hemicellulose degradation ratio (%)	Lignin degradation ratio (%)	Initial crude protein concentration (%)	The end of the crude protein concentration (%)
T1	30.0 ± 0.27	27.0 ± 1.59	−1.34 ± 0.10	12.0 ± 1.60	18.1 ± 0.50
T2	29.8 ± 1.32	23.6 ± 1.74	−0.95 ± 0.05	11.2 ± 2.62	17.2 ± 2.01
T3	36.4 ± 3.95	16.5 ± 2.35	2.25 ± 0.05	12.1 ± 0.57	16.1 ± 0.69
T4	34.6 ± 0.68	15.7 ± 1.26	1.35 ± 0.34	9.9 ± 1.92	16.5 ± 0.62

single-substrate AD group, and the cumulative CH_4 production of T3 (120 mL·g^{-1} per VS) was also higher than that of T4 (96.7 mL·g^{-1} per VS). This further confirmed that the CH_4 production potential of the FCS system was higher than that of the DCS system.

It noticed that the CH_4 production of the co-digestion was lower than that of the single-substrate AD group. For the single-substrate AD group, the reaction system was in a stable state, and the available organic compound of straw (86.4% VS fresh material and 85.3% VS dry material) was higher than that of cattle manure (16.9% VS). Under the conditions of specific reaction volume and substrate concentration, the addition of cattle manure in co-digestion reduced the total amount of organic compound available in the reaction system. In a word, FCS had better methanogenic potential than DCS.

3.2   Physical and chemical characteristics

3.2.1   Analysis of surface microstructure changes

SEM is one of the effective ways for observing physical structure changes of materials[26]. SEM analysis was conducted to further explore the relationship between micro-surface

structure and methanogenic potential of fresh and DCS. The results were shown in Fig. 2(a,b). The FCS surface become crinkled rough and uneven, while the DCS surface texture was full and tidy. During the production of FCS, the excess water inside corn straw directly sublimates, and the surface of water ice crystallization had folds and curls, but the pore and fissure structure were retained[27], resulting in loose and porous physical structure[28]. However, for the DCS, natural dehydration process leads to tissue contraction and cell collapse deformation, which was consistent with the study of Wan et al.[29]. This indicates that FCS is easily degraded by microbes, thereby effectively enhancing the methane production process[30, 31].

3.2.2   FTIR analysis

FTIR can be used to characterize the groups and chemical bonds intuitively[32]. Figure 2(c) shows the change curve from wave number 400–4000 cm^{-1}. It is clear that the characteristic absorption peaks of infrared spectra of the two corn straw were the same, 1420 and 1370 cm^{-1} were related to aromatic ring and C-H bond vibration in lignin respectively[32, 33], and there was no significant change in the two characteristic absorption peaks, indicating that lignin in the two kinds of corn straw was
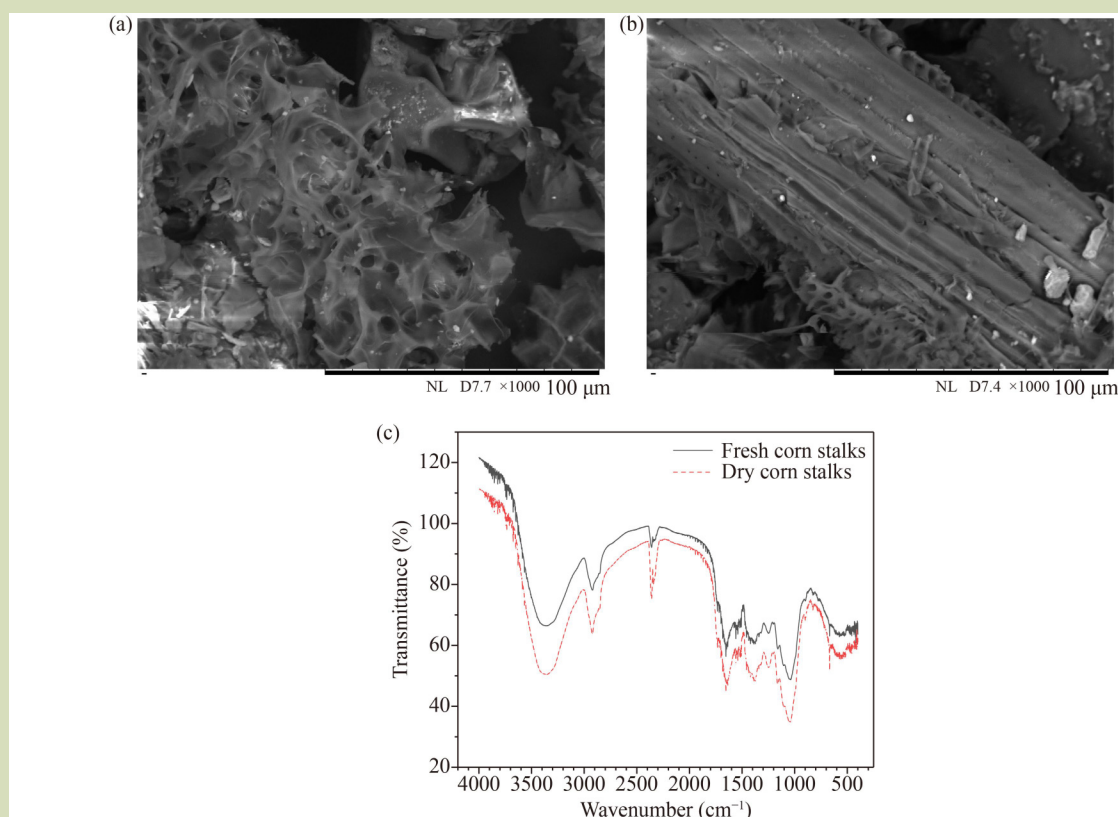
Fig. 2 Results of surface microstructure changes. (a) Scanning electron microscope images of fresh corn straw (×1000); (b) scanning electron microscope images of dry corn straw (×1000); (c) fourier transform infrared spectrum of corn straw.

basically unchanged. No significant changes in the chemical group in the components were found and there was no contribution to the otherness of methane production between fresh and DCS.

3.2.3 Mechanical properties analysis

The mechanical properties of corn straw have a direct relationship with the internal structure[34]. In order to explore the relationship between the internal structure changes of corn straw and its CH_4 production potential, the elastic modulus of corn straw was analyzed. Table 2 indicates that the elastic modulus of the dried corn straw was 5.76 MPa, which was about 3.47 times that of the FCS. This shows that the intermolecular structure of the dry material is more compact, the tensile stress is large, and the molecular structure is not easily destroyed. The structure of FCS is relatively loose, and the degree of intermolecular polymerization is not high. This shows that the fiber structure of FCS is more easily degraded.

In conclusion, there was no significant difference between the two types of corn straw in terms of structural composition (the

FTIR analysis shown). The main difference is that the FCS itself is not dense and hard (the results of SEM and mechanical property), and it is more easily degraded and transformed by microorganisms. This is an important reason for the higher CH_4 production potential of FCS.

3.3 Anaerobic digestion performance and intermediate metabolites

3.3.1 VFAs, pH, TAN and FAN analysis

In order to reveal the internal reasons for the difference in CH_4 production between fresh and DCS HS-AD system, the AD performance was analyzed via VFAs, pH, TAN and FAN as shown in Fig. 3(a–d). The pH of each group was maintained between 5.95 and 8.50 (Fig. 3(a,b)). For the single-substrate AD group, large amounts of acetic acid and butyric acid (15.7 and 3.42 g·L^{-1}, respectively) produced in T1 on day 4. At that time, the pH was 6.02, which was lower than the suitable pH range (6.8–7.5) for most methanogenic archaea[35], resulting in a short-term acidification of the system. With the progress of the digestion reaction, the acidification
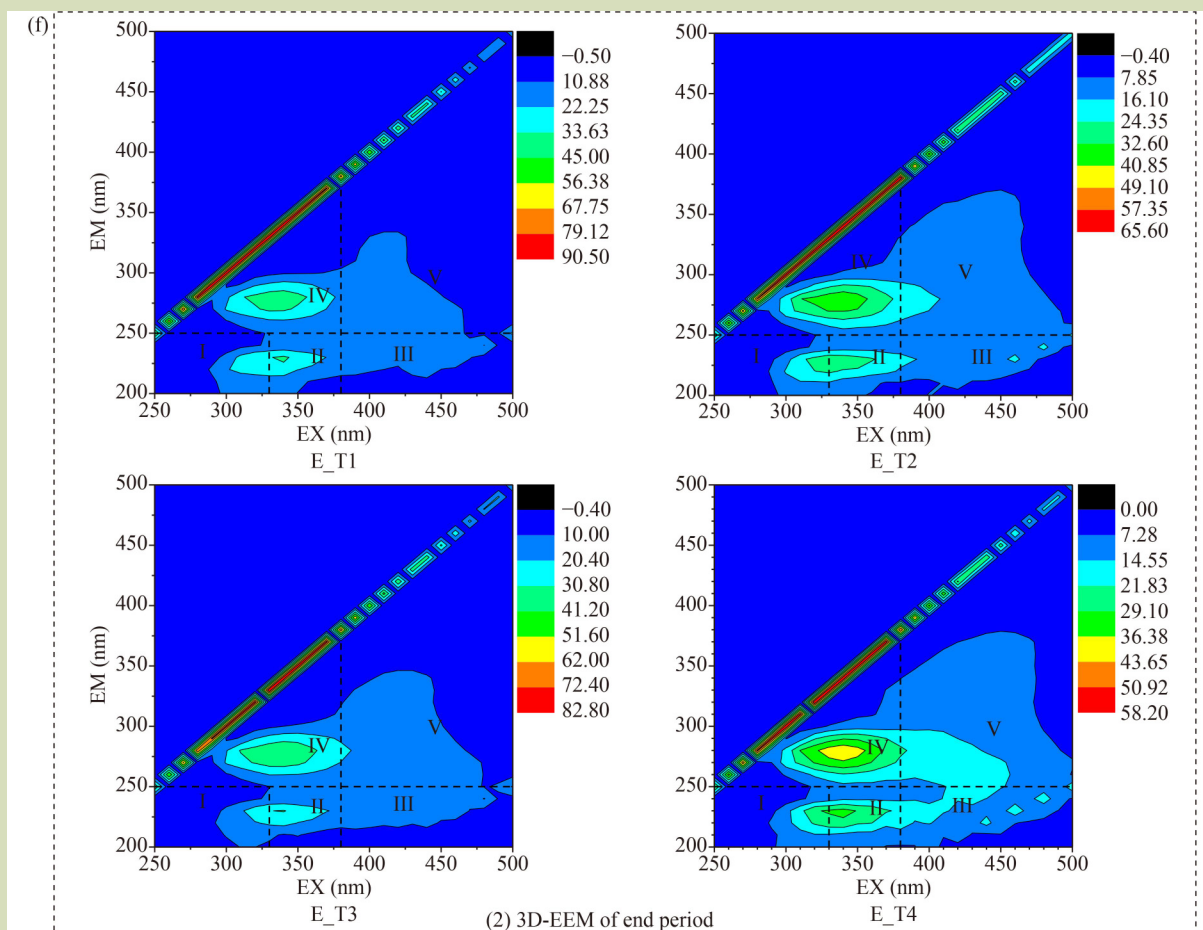
(1) 3D-EEM of stable period
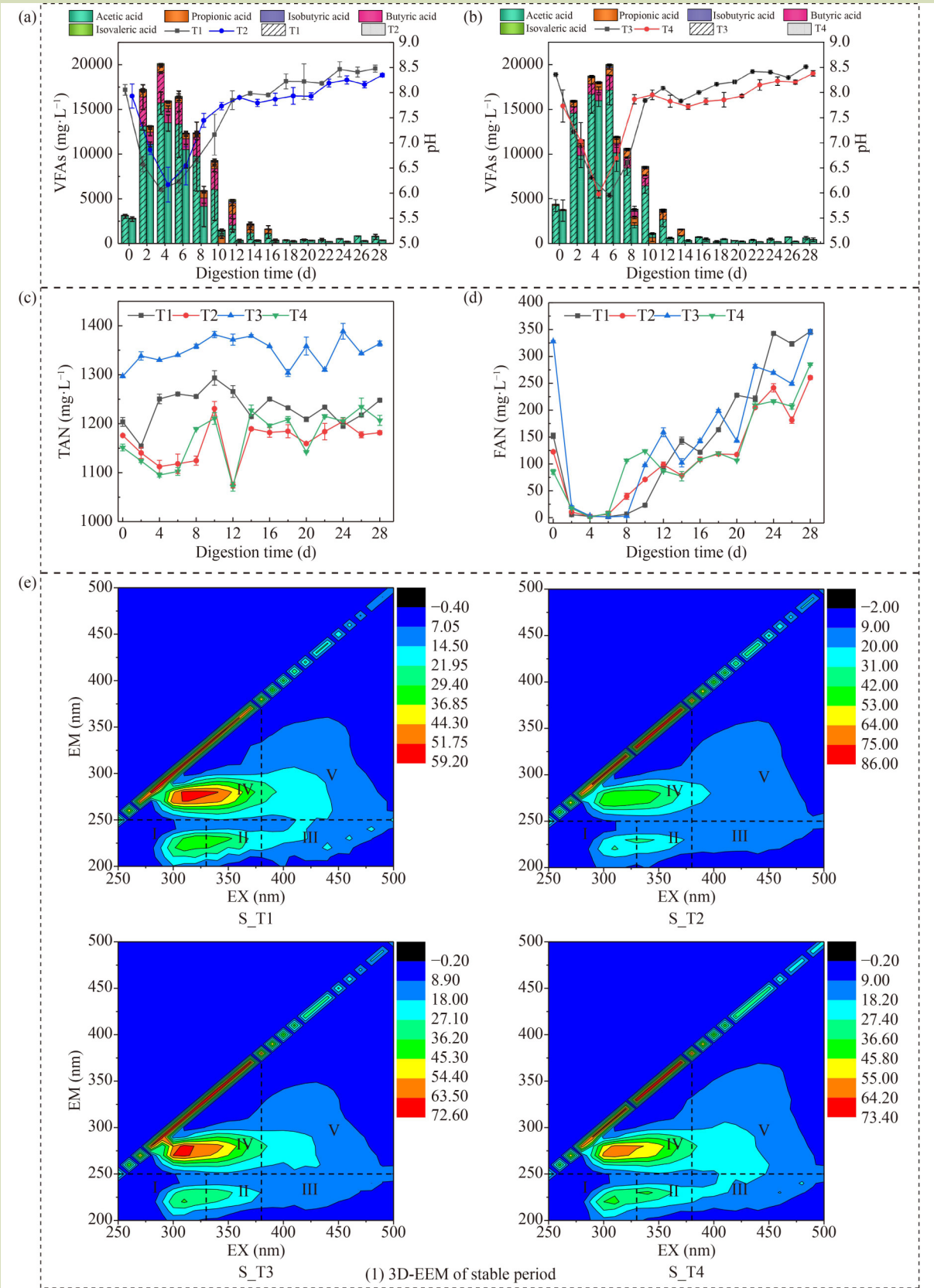
Fig. 3 Analysis of intermediate metabolites. (a) VFAs, T1 and T2; (b) VFAs, T3 and T4; (c) TAN; (d) FAN; (e) 3D-EEM of stable period; (f) 3D-EEM of end period.

phenomenon gradually alleviated due to the regulation of HS-AD system itself. Propionic acid accumulated on day 12 (1.19 g·L^{-1}). With the decrease of hydrogen partial pressure, the accumulated butyric acid and propionic acid were gradually degraded into acetic acid[36], and acetic acid was quickly utilized by methanogens. Therefore, the pH gradually increased and remained at about 7.7 over the following 4 days. T2 contained the same kinds of VFAs as T1, but the overall concentration was less than T1. Acetic acid and butyric acid reached their peaks on day 4 (13.5 and 1.58 g·L^{-1}, respectively). Compared with T1, acetic acid decreased by 14.2% and butyric acid decreased by 53.3% during the same period. The propionic acid reached its peak on day 10 (735 mg·L^{-1}) and was less than T1. After day 12, only acetic acid remained at a low level and was less than T1. For the co-digestion group, the VFAs of T3 for each stage of AD process was higher than that of T4, the trends of which was similar to that of the single-substrate AD group. The results showed that in the HS-AD process, acetic acid was the main component of VFAs in each digestion

system, followed by butyric acid and propionic acid. The appropriate concentration of VFAs could provide sufficient substrate for methanogens[37]. In this study, whether it was the single-substrate AD group or the co-digestion group, compared to the DCS, the FCS had a temporary acidification phenomenon, which affected the daily CH$_4$ production and led to the peak time lags as indicated above. Overall, compared with the DCS, the higher concentration of VFAs as the main precursor in the FCS contributed to the higher methanogenesis potential.

In addition, the ammonia nitrogen (TAN) concentration more than 3.0 g·L^{-1} and free ammonia (FAN) concentration more than 1.70 g·L^{-1} have been reported to inhibit an AD system[38]. The TAN concentration of each treatment group was in the range of 1.05–1.40 g·L^{-1} (T3 > T1 > T4 > T2). The concentration of FAN decreased rapidly on the day 2, and then increased, but the highest concentration did not exceed

412

Front. Agr. Sci. Eng. 2023, 10(3): 403–423

350 mg·L^{-1} (Fig. 3(c,d)), indicating that no inhibition occurred in the HS-AD system.

3.3.2 Metabolism characteristics of soluble organic compound

The 3D-EEM fluorescence spectroscopy technology can be used to analyze the soluble organic compound in samples based on the spectral characteristics[39]. Generally the 3D-EEM spectra of digestion supernatant can be divided into five regions based on the specific ranges of Ex and Em wavelength, which represents five types of organics: tyrosine-like proteins (Region I), tryptophan-like (Region II), fulvic acid-like (Region III), soluble microbial byproducts (Region IV) and humic acid-like (Region V) substances. Among these organics, tyrosine-like proteins (Region I) and soluble microbial byproducts (Region IV) are considered as biodegradable substrates, while tryptophan-like, fulvic acid-like and humic acid-like substances (Regions II, III and V) are regarded as the non-biodegradable substrates[40]. As shown in Fig. 3(e,f), during the stable period of methanogenesis, the fluorescence peaks of samples from the single-substrate AD mainly appeared in Regions I, II and IV, and there were significant differences in Regions I and IV. The fluorescence peaks of tyrosine-like proteins (Region I) and soluble microbial byproducts (Region IV) in S_T1 were higher than that in S_T2, indicating that there were more proteins and other degradable organics in the FCS HS-AD system.

Similarly, for the co-digestion system, the fluorescence peaks of Regions I and IV in S_T3 were higher than in S_T4. From the stable stage to the final stage of AD process, the protein and dissolved organics from substrates were gradually degraded and utilized by microorganisms. At the end of CH$_4$ production, the dissolved metabolites in E_T3 (Region IV) were less than that in E_T4 during the same reaction time. The results indicated that the degradation ratio of organic compound in the FCS HS-AD system was higher. It could be inferred that the concentration of microbial metabolites such as crude protein, small molecular organic acids in the FCS system was higher than that of the DCS system, which was conducive to the improvement of CH$_4$ production efficiency.

3.4 Trends in microbial evolution
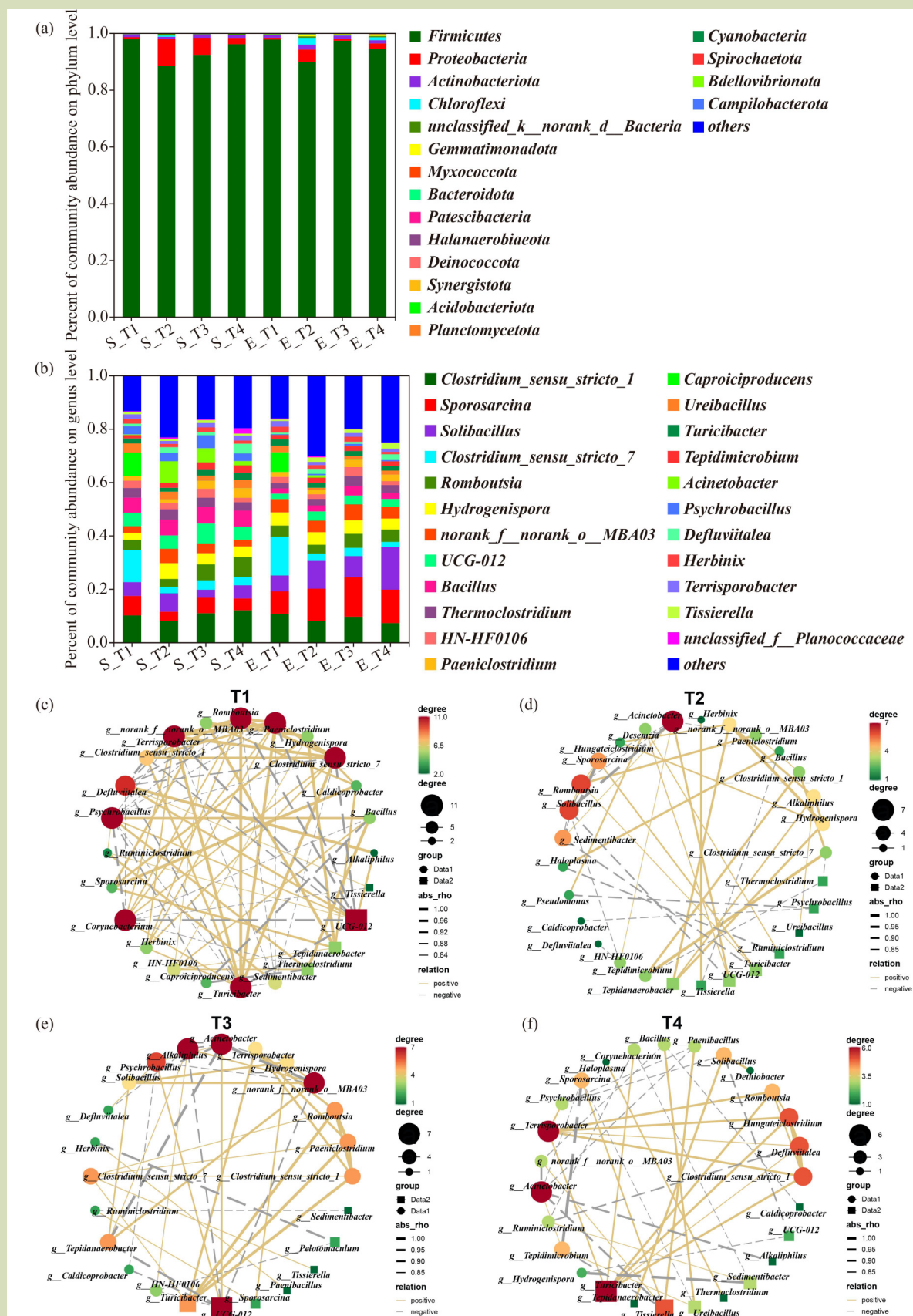
3.4.1 Bacterial community

The composition and diversity of the bacterial community in the stable and the end stages of HS-AD were characterized. As can be seen in Table 4, the effective sequence coverage of each samples in all test groups exceeded 98%, indicating that the bacterial gene sequence detection ratio was high, which can represent the true situation of the bacterial communities. Compared with the Shannon and Chao1 indices in the FCS HS-AD system, the DCS HS-AD system (T2 and T4) had higher abundance during the stable and the end phase of HS-AD. Simpson index (S_T1 > S_T2, E_T1 > E_T2, S_T3 > S_T4, E_T3 > E_T4) indicated that the DCS HS-AD system had a more uniform bacterial community. The different test between index groups was shown in Fig. S1.

From the perspective of community composition (Fig. 4(a)), the relative taxonomic abundance of bacterial communities in all samples accounted for at least 0.01% of the total. At the phylum level, each group was dominated by Firmicutes and Actinobacteriota, which were considered to be the core microorganisms in the hydrolysis and acidification stages of AD system, respectively[41]. The proportion of different microorganisms in each group of samples was different. In this study, the bacterial microbial composition of the single-substrate FCS HS-AD was specific, reflecting the greatest distance in the principal component analysis (PCA). The

Table 4 Bacterial microbial diversity index table in different samples

Sample	Shannon	Simpson	ACE	Chao1
S_T1	0.83 ± 0.26	0.59 ± 0.15	35.2 ± 1.97	33.9 ± 1.81
S_T2	1.41 ± 0.04	0.32 ± 0.01	37.1 ± 1.16	36.8 ± 0.75
S_T3	1.25 ± 0.02	0.42 ± 0.01	33.1 ± 0.91	32.9 ± 1.12
S_T4	1.16 ± 0.04	0.40 ± 0.01	38.3 ± 1.79	34.7 ± 0.42
E_T1	1.40 ± 0.01	0.34 ± 0.00	39.4 ± 1.46	39.5 ± 1.77
E_T2	1.54 ± 0.15	0.33 ± 0.03	50.1 ± 2.54	46.5 ± 0.92
E_T3	1.32 ± 0.00	0.36 ± 0.00	38.9 ± 1.70	38.1 ± 1.47
E_T4	1.48 ± 0.02	0.33 ± 0.00	44.7 ± 0.85	45.1 ± 1.25

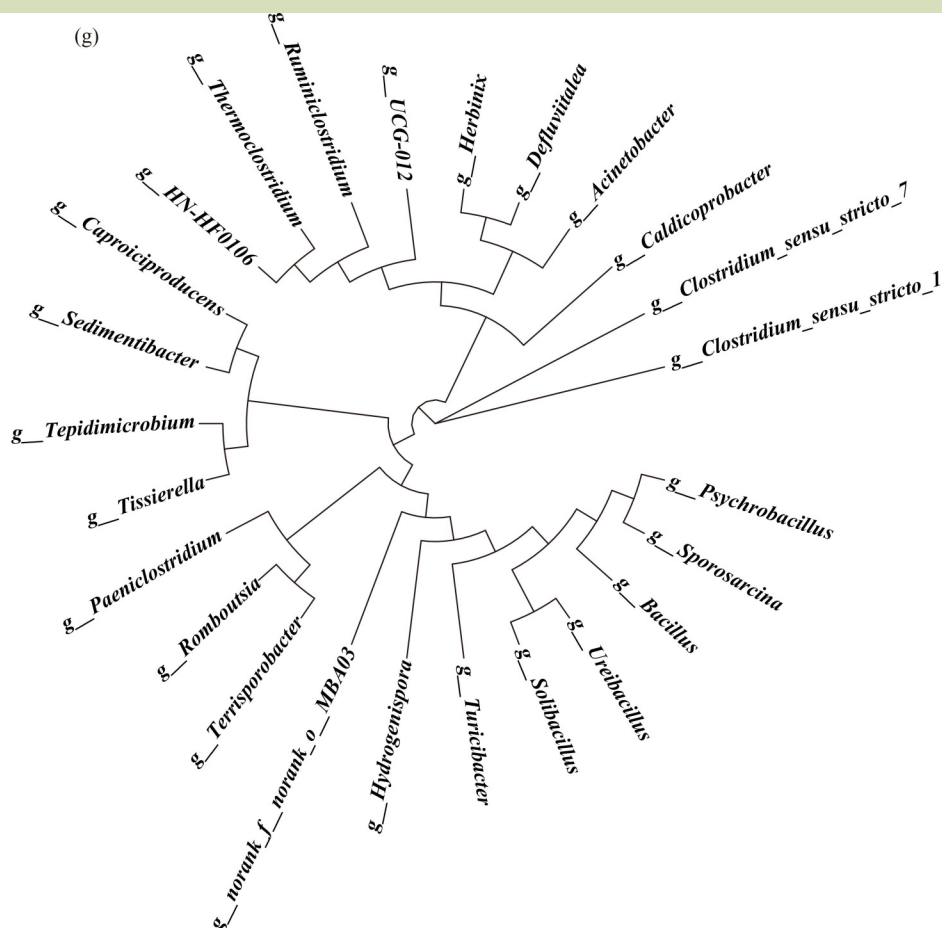Note: Coverage for all samples was 1.00 ± 0.00.

Fig. 4 Bacterial community evolution. (a) Bacterial community structure at phylum level; (b) bacterial community structure at genus level; (c–f) bacterial coexistence patterns in the T1–T4 digestive system, respectively (circle size/color depth represent the number of related objects; line type/color represent positive and negative correlations, solid lines represent positive correlations and dotted lines represent negative correlations; line thickness represents the size of the correlation coefficient, thicker lines indicate that the species are more closely related); (g) phylogenetic tree on genus level of T1/T2/T3/T4.

species composition of the co-digestion group was similar, which was reflected in the closer distance in the PCA (Fig. S2(a,b)).

In the stable period of single-substrate AD, the relative abundance of Firmicutes in S_T1 was 10.7% higher than S_T2 (S_T1 97.9% and S_T2 88.4%). Firmicutes can produce extracellular enzymes, such as cellulase, lipase, protease and and others, which are important in the catabolism of organic compounds[42]. Combined with the substrate degradation characteristics (see Section 3.1), the concentration of intermediate metabolites in T1 was much higher than that of T2 due to the role of Firmicutes. Actinobacteriota (S_T1 1.0% > S_T2 0.8%) was not highly abundant in the two HS-AD systems. Actinobacteriota could degrade cellulose into acetic acid or propionic acid[43], which was the reason the

concentration of propionic acid in the FCS system was higher than in the DCS (see Section 3.2.1). For the co-digestion group, the relative abundance of Firmicutes in the stable phase was different from that in single-substrate AD. The FCS system (S_T3 92.4%) was less than the DCS system (S_T4 96.1%). The relative abundance of Actinobacteriota in FCS system was still higher than that of DCS system (S_T3 1.2% and S_T4 0.9%), which showed that microorganisms responded differently as environmental conditions change. As the organic compound was utilized completely in the end stage of HS-AD, the diversity and activity of microorganisms were relatively reduced.

The coordination of key bacteria is critical for the process of hydrolysis and acidification in AD system. Therefore, the genus-level correlation network analysis (Fig. 4(c–f)) and

function prediction (Fig. 4(g)) of bacterial communities for the four HS-AD groups were performed. It can be found that in the single-substrate AD group, *Clostridium_sensu_stricto_1* (S_T1 10.1% and S_T2 8.0%) and *Clostridium_sensu_stricto_7* (S_T1 12.1% and S_T2 2.4%) were core bacteria, which jointly participate in the degradation of proteins and polysaccharides[44,45]. *Sporosarcina* is a microorganism that degrades low-molecular compounds. The close relationship between *Sporosarcina* (S_T1 7.3% and S_T2 3.5%) and *Psychrobacillus* (S_T1 3.2% and S_T2 3.1%) was shown in Fig. 4(g). It is speculated that the two participated in the degradation of low-molecular compounds in the AD system. The relative abundance of *UCG-012* (S_T1 5.1% and S_T2 5.0%) and *HN-HF0106* (S_T1 2.8% and S_T2 2.4%) in the FCS system was higher than that in the dry system, but the functions of these two microorganisms have not been identified. In view of the fact that *Ruminiclostridium, UCG-012* and *HN-HF0106* were closely related among the three microorganisms (Fig. 4(g)). Also, *Ruminiclostridium* is a unique microorganism that degrades cellulose and xylan under high temperature conditions[46]. They participate in the reaction process together to increase the degradation ratio. It is noteworthy that all the important bacterial genera mentioned above belong to Firmicutes, (e.g., *Thermoclostridium, UCG-012* and *HN-HF0106*), which dominated the interaction of the system and cooperate with other bacterial genera to complete the degradation (Fig. 4(c,d)). Also, the relative abundance of S_T1 was always higher than that of S_T2, which had a certain positive correlation with the high concentration of intermediate metabolites in the FCS system, including the concentration of VFAs and the concentration of soluble organic compound. It shows that the single-substrate FCS HS-AD group has a strong ability to transform and metabolize intermediate metabolites, which is related to the difference in CH$_4$ production potential between fresh and DCS system. All the bacterial genera mentioned above also existed in the co-digestion group(S_T3 > S_T4, from the relative abundance of species), including *Clostridium_sensu_stricto_7* (S_T3 3.5% and S_T4 3.1%), *Sporosarcina* (S_T3 5.8% and S_T4 4.4%), *Psychrobacillus* (S_T3 4.9% and S_T4 2.8%) and *UCG-012* (S_T3 7.5% and S_T4 4.9%). Combined with the analysis of intermediate metabolites, it is further verified that the FCS system had a strong ability to metabolize intermediate metabolites, resulting in a higher CH$_4$ production efficiency than that of the DCS system. In addition, by comparing with the single-substrate AD group and the co-digestion group, *Tepidimicrobium* (belonging to Firmicutes) in T3 had a clear competitive relationship with other bacteria (Fig. 4(e)), which severely limited the function of other bacteria and weakened the intermediate metabolism of organic matter, in turn

inhibiting the CH$_4$ production process. This might be directly related to the inferior CH$_4$ production potential of this system compared to T1. *Acinetobacter* (belonging to Proteobacteria) in T4 had a strong synergistic effect with other bacteria. This is an extreme function of heterotrophic nitrification and aerobic denitrification resistant to high ammonia nitrogen. Its role is to degrade organic compound and remove nitrogen[47]. However, the relative abundance of *Acinetobacter* in the co-digestion group was relatively low (S_T4 1.6%), which could not effectively promote the function of other bacteria and was not conducive to the production of intermediate metabolites, resulting in lower CH$_4$ production potential than T2.

Compared with the FCS system (T1 and T3), the bacterial community diversity in the DCS system (T2 and T4) was higher. However, the bacterial function expression of the DCS system was inhibited. This shows that *Clostridium_sensu_stricto_1, Clostridium_sensu_stricto_7, Sporosarcina, UCG-012* and others (belonging to Firmicutes) have obvious synergistic effects with other bacteria, increasing the production and metabolic ratio of intermediate metabolites, which provide conditions for methanogenesis. However, the relative abundance of related bacteria in the DCS system (T2 and T4) was relatively small and could not effectively cooperate with other microorganisms, which negatively affected the conversion of intermediate metabolites and weaken the activity of methanogenesis. This is the main reason for the difference in CH$_4$ production potential between FCS and DCS systems.

3.4.2 Archaeal community

Compared with bacteria, archaea are the direct contributor to CH$_4$ production. The diversity index was used to evaluate the archaeal alpha diversity of samples (Table 5). The difference test between index groups is shown in the supplementary materials (Fig. S1). The effective sequence coverage of all samples exceeds 98%, indicating that the detection ratio of archaeal gene sequence in samples was high, which could represent the true situation of archaeal community. Shannon index and Chao1 index (S_T1 > S_T2, E_T1 > E_T2, S_T3 > S_T4, E_T3 > E_T4) showed the diversity and richness of archaeal community in the FCS system (T1, T3) were higher than that in the DCS (T2, T4). The Simpson index (S_T1<S_T2, E_T1<E_T2, S_T3<S_T4, E_T3<E_T4) indicated that the archaeal community in the FCS system was more uniform than that in the DCS.

The characteristics of the archaeal community structure in the stable and end stages were analyzed. Figure 5(a,b) shows the relative taxonomic abundance of archaeal communities at

Table 5   Archaea microbial diversity index table in different samples

Sample\Estimators	Shannon	Simpson	ACE	Chao1
S_T1	0.87 ± 0.14	0.49 ± 0.04	14.4 ± 2.79	14.0 ± 2.83
S_T2	0.64 ± 0.02	0.59 ± 0.02	9.0 ± 0.41	8.7 ± 0.38
S_T3	0.69 ± 0.03	0.55 ± 0.02	10.2 ± 7.20	16.0 ± 3.54
S_T4	0.67 ± 0.02	0.59 ± 0.03	8.8 ± 0.70	8.3 ± 0.51
E_T1	0.70 ± 0.00	0.56 ± 0.03	27.5 ± 0.01	14.3 ± 2.65
E_T2	0.69 ± 0.02	0.57 ± 0.02	9.6 ± 0.26	9.3 ± 0.19
E_T3	0.69 ± 0.00	0.54 ± 0.01	39.9 ± 11.13	15.0 ± 0.71
E_T4	0.67 ± 0.02	0.58 ± 0.02	10.6 ± 1.12	9.2 ± 0.42

Note: Coverage for all samples was 1.00 ± 0.00.

genus level. The diversity of archaeal communities in the FCS system (T1 and T3) was higher than that in the DCS system (T2 and T4). The archaeal communities identified in the four HS-AD groups were similar in structure. In particular, the single-substrate AD of FCS was specific. Since the distance among the samples in the PCA diagram was the farthest (Fig. S2(c,d)). All groups were mainly *Methanosarcina*, *Methanoculleus*, *Methanobrevibacter* and *Methanomassiliicoccus*. The first three archaea belong to Euryarchaeota. *Methanomassiliicoccus* is a new branch of methanogens that evolved independently in the phylogeny[48,49]. These four types of microorganisms are considered to be the core microorganisms of the methanogenic system. In the single-substrate AD group, *Methanosarcina* had the highest relative abundance in the stable stage; S_T1 (54.4%) was 22.6% less than S_T2 (70.2%). This is a multifunctional methanogen, it can produce CH_4 through three types of pathways: hydrogenotrophic, acetotrophic and methylotrophic. It is the only archaea that can produce CH_4 through these pathways. *Methanosarcina* has been found to have a high tolerance to VFAs and OLR[50,51]. When the TAN concentration in the reactor rose to 3.0 $g·L^{-1}$ or the acetic acid concentration reached 3.0 $g·L^{-1}$, the CH_4 generation pathway of the AD system would change from acetoclastic reaction to hydrogenotrophic. In this study, a large amount of acetic acid accumulated in the system, far more than 3.0 $g·L^{-1}$. Therefore, it is speculated that *Methanosarcina* mainly used the hydrogenotrophic pathways to produce CH_4. It is also noteworthy that *Methanoculleus* (S_T1 26.5% and S_T2 28.9%) and *Methanobrevibacter* (S_T1 17.6% and S_T2 0.2%), as the second and third most abundant microbial communities, were both hydrogenotrophic methanogens. They mainly used H_2 and CO_2, or formic acid to generate CH_4. They are more tolerant to environments with high organic loads[52].

Compared with *Methanosarcina* and *Methanoculleus* in FCS system, the relative abundance of *Methanobrevibacter* was higher and had a positive correlation with CH_4 production. In the stable period of the co-digestion group, the *Methanosarcina* of S_T3 (65.8%) was 9.2% less than that of S_T4 (72.5%), which was consistent with the relative abundance trend of the single-substrate AD group. In the co-digestion group, the *Methanoculleus* of S_T3 (32.7%) was 7.3% higher than that of S_T4 (24.6%). The *Methanobrevibacter* of S_T3 (0.8%) was higher than that of S_T4 (0.6%), the trend of the proportion in the FCS system and the DCS system was same to that of the single-substrate AD group. The relative abundance of *Methanomassiliicoccus* of S_T3 (0.6%) was 72.7% lower than that of S_T4 (2.2%). *Methanomassiliicoccus* is a methylotrophic methanogen, which mainly uses methanol or methylamine and hydrogen as electron donors to produce CH_4[53,54].

Correlation network analysis and function prediction were performed on the archaeal communities of the four HS-AD groups at genus level (Fig. 5(c–f)). The main methanogenic archaea were *Methanosarcina, Methanoculleus, Methanobrevibacter,* and *Methanomassiliicoccus.* There was a synergistic effect between *Methanosarcina* and other archaea in T1, and the activity was the highest. However, *Methanoculleus* and *Methanobrevibacter* had a competitive relationship with other archaea, competing for nutrients such as H_2 and CO_2, or formic acid. Due to the strong adaptability of these two microorganisms to the environment[52,55], T1 maintained an ample CH_4 production potential. However, most of these key microorganisms were in competition with other archaea in T2, which meant that under limited environmental conditions, CH_4 conversion was limited. For this reason the CH_4 production potential for the single-substrate AD of FCS was greater than that of DCS.
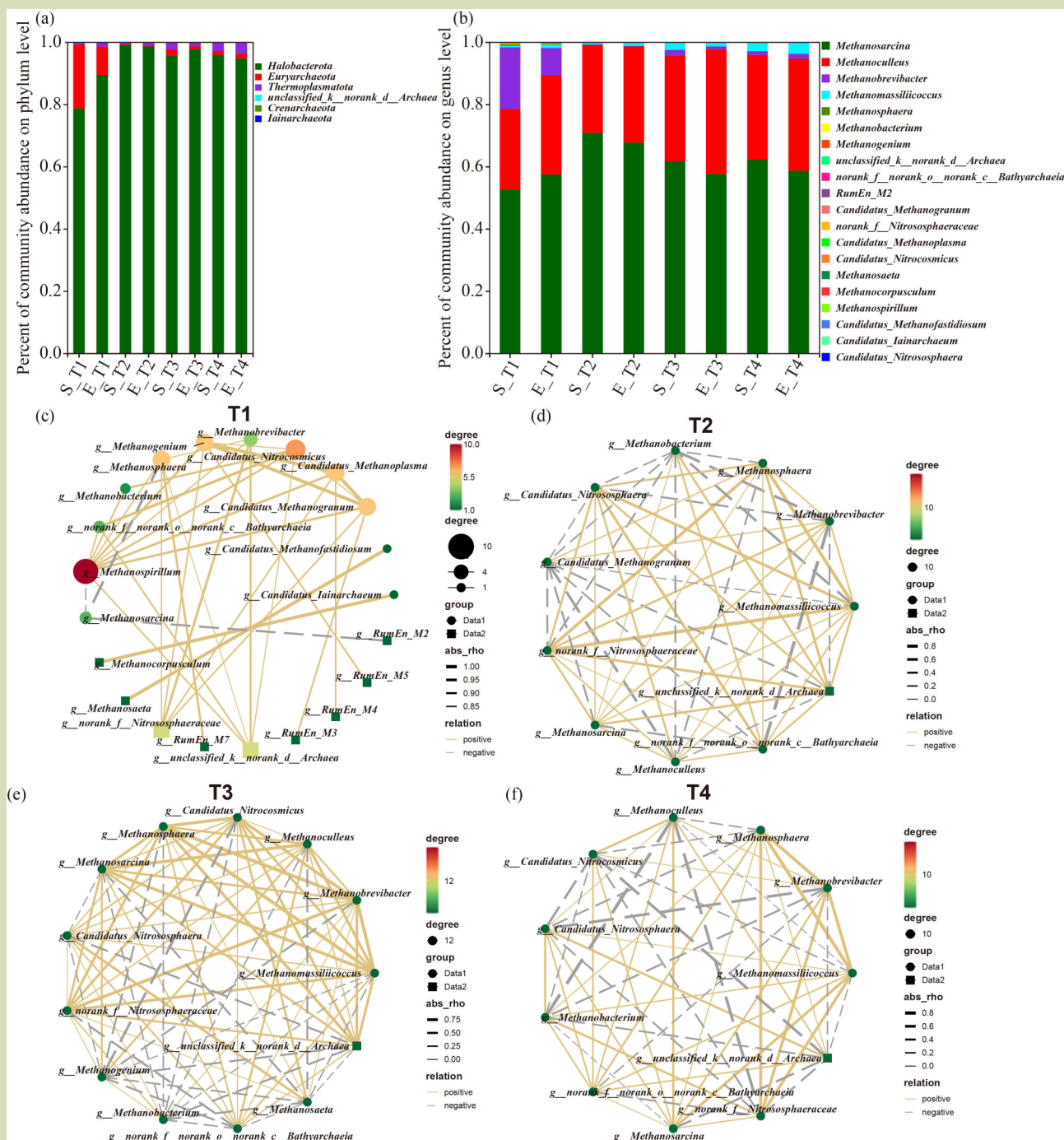
Fig. 5 Archaea community evolution. (a) Archaea community structure at phylum level); (b) archaea community structure at genus level; (c–f) archaea coexistence patterns in the T1–T4 digestive system, respectively (circle size/color depth represent the number of related objects; line type/color represent positive and negative correlations, solid lines represent positive correlations and dotted lines represent negative correlations; and line thickness represents the size of the correlation coefficient, thicker lines indicate that the species are more closely related).

3.5 Metagenomic analysis

Based on the above analysis of the intermediate metabolites and microbial community composition of the four HS-AD

groups, the microbial interactions and metabolic pathways of the dominant species could be significantly different. Thus, metagenomics analysis was performed to explore the deep-

418

Front. Agr. Sci. Eng. 2023, 10(3): 403–423

seated reasons for the differences in the metabolic pathways of microorganisms.

By comparing with the KEGG ortholog (KO) database, the metabolic pathways of microbial community were determined. For each group of metagenomics, genes encoding metabolic functions were dominate, accounting for more than 60% of each sample, which were T1 65.6%, T2 67.6%, T3 67.1% and T4 68.3%. Followed by genetic information processing (T1 12.3%, T2 11.7%, T3 11.8% and T4 11.9%) and environmental information processing (T1 8.6%, T2 7.9%, T3 8.2% and T4 7.6%) (Fig. 6(a)). In the single-substrate AD group, the most abundant type of metabolism was carbohydrate metabolism (T1 14.8% and T2 14.6%). The abundance of the T1 genome was higher than that of T2, which indicated that the genes involved in carbon metabolism and CH_4 conversion in the FCS system were relatively highly expressed, leading to more CH_4 production. The gene abundance of nucleotide metabolism, glycan biosynthesis and metabolism was also T1 > T2, a high proportion of genes related to these functions had been previously reported in metagenomes[56–58], metatranscriptomes[59] and metaproteomes[60] in AD system, indicating these metabolic activities were linked to the conversion of carbohydrates to CH_4. In the co-digestion group, carbohydrate metabolism was T3 > T4 (T3 14.9% and T4 14.6%), which was particular to nucleotide metabolism and glycan biosynthesis and metabolism. These were necessary process for microorganisms to synthesize CH_4. The relative abundance of microorganisms involved in this process is beneficial for methane synthesis. The results showed that the T3 system was more favorable for CH_4 production than the T4 system, thus confirming the CH_4 production advantage of FCS over DCS. The annotation result of the methanogenic gene indicates three types of methanogenic pathways: hydrogenotrophic, acetotrophic, and methylotrophic (Fig. 6(b)). For hydrogenotrophic methanogenesis, CO_2 is successively reduced to CH_4 through a series of intermediates with a methyl group. The methyl group is then transferred to coenzyme M, forming methyl-CoM. Thus, methyl-CoM is reduced to CH_4 through methyl-coenzyme M reductase at the final step[61]. The genes involved in the hydrogenotrophic methanogenesis pathway had higher abundance, especially for formylmethanofuran dehydrogenase (K00200-K00203) and tetrahydromethanopterin S-methyltransferase (K00577-K00584). The abundance of each gene was upregulated in the FCS system (T1, T2), and downregulated in the DCS system (T2, T4) (Fig. 6(c)), it showed that there were more hydrogenotrophic pathways in the FCS HS-AD system. The gene of *Methanosarcina*, *Methanoculleus* and *Methanobrevibacter* included almost all the enzymes for

hydrogenotrophic pathway, indicating that archaea related to these three microorganisms tend to use hydrogen to convert CO_2 into CH_4, which has been shown with genomic and physiological data[62,63]. Through further screening and analysis, we found that *Methanoculleus* and *Methanobrevibacter* were strictly hydrogenotrophic methanogenic microorganisms, while *Methanosarcina* was a multifunctional methanogen, and the hydrogenotrophic pathway was found to mainly product CH_4 under the conditions of thermophilic and high VFAs. This confirmed the the speculation of the function of microorganisms (see Section 3.4.2).

In each treatment group, for *Methanosarcina*, in addition to the genes involved in the hydrogenotrophic pathway (mentioned above), genes involved in acetotrophic and methylotrophic pathways were detected. For the acetotrophic methanogenesis pathway (Fig. 6(b)), the gene encoding acetyl-CoA synthetase (K01895) is present in all reaction systems. Also, genes encoding phosphate acetyltransferase (K00625 and K13788) and acetate kinase (K00925) existed at the same time. These two genes were responsible for transforming acetate into acetyl phosphate and CoA into acetyl-CoA, respectively. It is noteworthy that the abundance of genes encoding the acetotrophic methanogenesis pathway was relatively low, especially K13788, so the acetotrophic pathway only weakly contributes to the CH_4 production process of this system. For the methylotrophic pathway (Fig. 6(b)), methyl-coenzyme M is the key enzyme for biological CH_4 formation[64]. Genes encoding the three subunits of methyl-coenzyme M reductase exist in the AD system: methanol-5-hydroxybenzimidazolylcobamide Co-methyltransferase [EC:2.1.1.90] (k04480), methanol corrinoid protein (k14080), [methyl-Co (III) methanol-specific corrinoid protein] and coenzyme M methyltransferase [EC:2.1.1.246] (k14081). This shows that *Methanosarcina* has the ability to convert methanol and methylamine to CH_4.

In addition, we found that *Methanomassiliicoccus* (k04480, k14080, k14081) also contained all the enzymes for the complete methylotrophic pathway, indicating that this microorganism can only produce CH_4 through a methylotrophic metabolic pathway, which was consistent with genomic insights of *Methanomassiliicoccus* as a methylotroph[65].

4 CONCLUSIONS

The FCS system had the highest cumulative CH_4 production
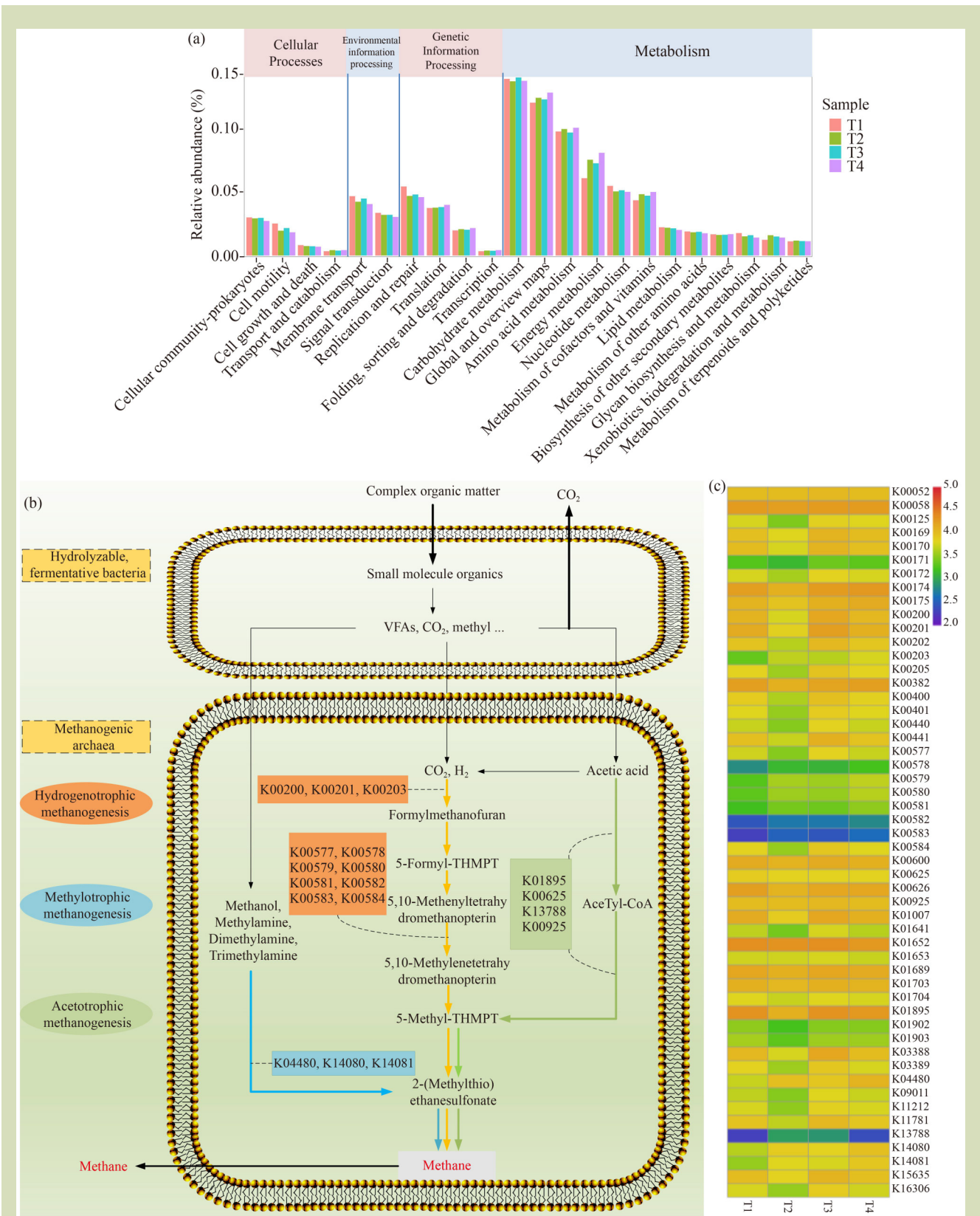
Fig. 6 Metagenomic results. (a) Relative abundances of the KEGG categories of functional genes in the metagenomes of the sample (KEGG level 1 and 2 description); (b) metabolic pathway diagram of methanogenesis of key genes; (c) relative abundances of the KEGG categories of functional genes.

420

Front. Agr. Sci. Eng. 2023, 10(3): 403–423

(144 mL·g^{-1} per VS), which was 7.5% higher than that of the DCS (134 mL·g^{-1} per VS). Firstly, compared with DCS, the surface structure of FCS was more conducive to cellulose degradation and it can contain more organic compounds for energy conversion. Secondly, the VS, crude protein concentration and cellulose degradation ratio were higher, which was positively correlated with the potential of CH$_4$ production. Thirdly, this was closely related to the metabolic activities of microorganisms in the process of HS-AD. *Clostridium_sensu_stricto_1* and *Clostridium_sensu_stricto_7* belonging to Firmicutes had a cooperative relationship with other bacteria and contributed to the acidification process. Methanogenic archaea adapted to the high acid in time, cooperated with microorganisms with different functions and converted intermediate products into CH$_4$ by using various nutritional pathways, such as acetate, hydrogen and methyl, including *Methanosarcina*, *Methanoculleus*, *Methanobrevibacter* and *Methanomassiliicoccus*. Among these, *Methanosarcina* was a multifunctional methanogen and contributed the most to hydrogenotrophic reactions to produce CH$_4$, effectively avoiding the inhibition of the CH$_4$ production process due to the excessive accumulation of VFAs. This study demonstrates that under the condition of thermophilic temperature and high OLR, the use of single-substrate HS-AD of FCS is a more reasonable way, which provides an important reference for regulating AD of crop straw with the purpose of high-efficiency CH$_4$ production

Supplementary materials

The online version of this article at https://doi.org/10.15302/J-FASE-2022471 contains supplementary materials (Figs. S1–S2).

Compliance with ethics guidelines

Jinzhi Huang, Xiaoting Yan, Zhen Liu, Mengyi Wang, Yangyang Hu, Zhenyu Li, Minsong Lin, and Yiqing Yao declare that they have no conflicts of interest or financial conflicts to disclose. This article does not contain any studies with human or animal subjects performed by any of the authors.

REFERENCES

1. Cheng Y, Awan U, Ahmad S, Tan Z. How do technological innovation and fiscal decentralization affect the environment? A story of the fourth industrial revolution and sustainable growth *Technological Forecasting and Social Change*, 2021, **162**: 120398

2. Kargbo H, Harris J S, Phan A N. "Drop-in" fuel production from biomass: critical review on techno-economic feasibility and sustainability. *Renewable & Sustainable Energy Reviews*, 2021, **135**: 110168

3. Panwar N L, Kaushik S C, Kothari S. Role of renewable energy sources in environmental protection: a review. *Renewable & Sustainable Energy Reviews*, 2011, **15**(3): 1513–1524

4. Bentsen N S, Felby C, Thorsen B J. Agricultural residue production and potentials for energy and materials services. *Progress in Energy and Combustion Science*, 2014, **40**: 59–73

5. Nguyen T, Hermansen J E, Mogensen L. Environmental performance of crop residues as an energy source for electricity production: The case of wheat straw in Denmark. *Applied Energy*, 2013, **104**: 633–641

6. Chandra R, Takeuchi H, Hasegawa T. Methane production from lignocellulosic agricultural crop wastes: a review in context to second generation of biofuel production. *Renewable & Sustainable Energy Reviews*, 2012, **16**(3): 1462–1476

7. Yu Q, Liu R, Li K, Ma R. A review of crop straw pretreatment methods for biogas production by anaerobic digestion in China. *Renewable & Sustainable Energy Reviews*, 2019, **107**: 51–58

8. Wang M, Zhou J, Yuan Y X, Dai Y M, Li D, Li Z D, Liu X F, Zhang X Y, Yan Z Y. Methane production characteristics and microbial community dynamics of mono-digestion and co-digestion using corn stalk and pig manure. *International Journal of Hydrogen Energy*, 2017, **42**(8): 4893–4901

9. Elalami D, Carrere H, Monlau F, Abdelouahdi K, Oukarroum A, Barakat A. Pretreatment and co-digestion of wastewater sludge for biogas production: Recent research advances and trends. *Renewable & Sustainable Energy Reviews*, 2019, **114**:

109287

10. Bedoić R, Spehar A, Puljko J, Cucek L, Cosic B, Puksec T, Duic N. Opportunities and challenges: experimental and kinetic analysis of anaerobic co-digestion of food waste and rendering industry streams for biogas production. *Renewable & Sustainable Energy Reviews*, 2020, **130**: 109951

11. Mussoline W, Esposito G, Lens P, Spagni A, Giordano A. Enhanced methane production from rice straw co-digested with anaerobic sludge from pulp and paper mill treatment process. *Bioresource Technology*, 2013, **148**: 135–143

12. Ghosh S, Chowdhury R, Bhattacharya P. Sustainability of cereal straws for the fermentative production of second generation biofuels: A review of the efficiency and economics of biochemical pretreatment processes. *Applied Energy*, 2017, **198**: 284–298

13. Zhao Y, Yu J, Zhao X, Zheng Z, Cai Y, Hu Y, Cui Z, Wang X. The macro- and micro-prospects of the energy potential of the anaerobic digestion of corn straw under different storage conditions. *Bioresource Technology Reports*, 2019, **7**: 100189

14. Meng Y, Jost C, Mumme J, Wang K J, Linke B. An analysis of single and two stage, mesophilic and thermophilic high rate systems for anaerobic digestion of corn stalk. *Chemical Engineering Journal*, 2016, **288**: 79–86

15. Wu L J, Qin Y, Hojo T, Li Y Y. Upgrading of anaerobic digestion of waste activated sludge by temperature-phased process with recycle. *Energy*, 2015, **87**: 381–389

16. Cavinato C, Fatone F, Bolzonella D, Pavan P. Thermophilic anaerobic co-digestion of cattle manure with agro-wastes and energy crops: comparison of pilot and full scale experiences. *Bioresource Technology*, 2010, **101**(2): 545–550

17. Hinken L, Urban I, Haun E, Urban I, Weichgrebe D, Rosenwinkel K H. The valuation of malnutrition in the mono-digestion of maize silage by anaerobic batch tests. *Water Science & Technology: A Journal of the International Association on Water Pollution Research*, 2008, **58**(7): 1453–1459

18. Mahdy A, Mendez L, Ballesteros M, Gonzalez-Fernandez C. Enhanced methane production of Chlorella vulgaris and Chlamydomonas reinhardtii by hydrolytic enzymes addition. *Energy Conversion and Management*, 2014, **85**: 551–557

19. Wei X, Jiang T, Li P, Liu K, Dong M. Anaerobic digestion capability of corn straw and cow manure by using lab-scale leach bed reactors system. *Chinese Journal of Environmental Engineering*, 2017, **11**(10): 5644–5650 (in Chinese)

20. Eaton A D, Clesceri L S, Rice E W, Greenberg A E, Franson M A H. Standard Methods for the Examination for Water and Wastewater. Washington, D.C: *American Public Health Association*, 2005

21. Ma J, Bashir M A, Pan J, Qiu L, Liu H, Zhai L, Rehim A. Enhancing performance and stability of anaerobic digestion of chicken manure using thermally modified bentonite. *Journal of Cleaner Production*, 2018, **183**: 11–19

22. You Z Y, Pan S Y, Sun N, Kim H, Chiang P C. Enhanced corn-stover fermentation for biogas production by NaOH pretreatment with CaO additive and ultrasound. *Journal of Cleaner Production*, 2019, **238**: 117813

23. Xu W, Fu S, Yang Z, Lu J, Guo R. Improved methane production from corn straw by microaerobic pretreatment with a pure bacteria system. *Bioresource Technology*, 2018, **259**: 18–23

24. Kanehisa M, Goto S. KEGG: Kyoto encyclopedia of genes and genomes. *Nucleic Acids Research*, 2000, **28**(1): 27–30

25. Xie C, Mao X, Huang J, Ding Y, Wu J, Dong S, Kong L, Gao G, Li C Y, Wei L. KOBAS 2.0: a web server for annotation and identification of enriched pathways and diseases. *Nucleic Acids Research*, 2011, **39**(Web Server issue): W316–W322

26. Dong L, Cao G, Zhao L, Liu B, Ren N. Alkali/urea pretreatment of rice straw at low temperature for enhanced biological hydrogen production. *Bioresource Technology*, 2018, **267**: 71–76

27. Ghaffar S H, Fan M. Structural analysis for lignin characteristics in biomass straw. *Biomass and Bioenergy*, 2013, **57**: 264–279

28. Tang H T, Wang F, Li W, Li A, Ha Y, Li Y. Effect of γ-rays irradiation and alkali solution pretreatment on hydrolyzing enzyme and microcosmic structure of core straw. *Journal of Nuclear Agricultural Sciences* (*He-Nong Xuebao*), 2012, **26**(3): 535–542 (in Chinese)

29. Wan T, Xiong L, Huang R, Zhao Q, Tan X, Qin L, Hu J. Structure and properties of corn stalk-composite superabsorbent. *Polymer Bulletin*, 2014, **71**(2): 371–383

30. Guo H, Chang J, Yin Q, Wang P, Lu M, Wang X, Dang X. Effect of the combined physical and chemical treatments with microbial fermentation on corn straw degradation. *Bioresource Technology*, 2013, **148**: 361–365

31. Wei Y, Wu D, Wei D, Zhao Y, Wu J, Xie X, Zhang R, Wei Z. Improved lignocellulose-degrading performance during straw composting from diverse sources with actinomycetes inoculation by regulating the key enzyme activities. *Bioresource Technology*, 2019, **271**: 66–74

32. Xu X, Xu Z, Shi S, Lin M. Lignocellulose degradation patterns, structural changes, and enzyme secretion by *Inonotus obliquus* on straw biomass under submerged fermentation. *Bioresource Technology*, 2017, **241**: 415–423

33. Bassilakis R, Carangelo R M, Wójtowicz M A. TG-FTIR analysis of biomass pyrolysis. *Fuel*, 2001, **80**(12): 1765–1786

34. Adapa P, Schoenau G, Tabil L, Sokhansanj S, Singh A. Compression of fractionated sun-cured and dehydrated alfalfa chops into cubes-specific energy models. *Bioresource Technology*, 2007, **98**(1): 38–45

35. Xu Y, Lu Y, Zheng L, Wang Z, Dai X. Perspective on enhancing the anaerobic digestion of waste activated sludge. *Journal of Hazardous Materials*, 2020, **389**: 121847

36. Chi X, Li J, Wang X, Zhang Y, Leu S Y, Wang Y. Bioaugmentation with *Clostridium tyrobutyricum* to improve butyric acid production through direct rice straw bioconversion. *Bioresource Technology*, 2018, **263**: 562–568

37. Viéitez E R, Ghosh S. Biogasification of solid wastes by two-

phase anaerobic fermentation. *Biomass and Bioenergy*, 1999, **16**(5): 299–309

38. Jiang Y, McAdam E, Zhang Y, Heaven S, Banks C, Longhurst P. Ammonia inhibition and toxicity in anaerobic digestion: a critical review. *Journal of Water Process Engineering*, 2019, **32**: 100899

39. Chen W, Westerhoff P, Leenheer J A, Booksh K. Fluorescence excitation-emission matrix regional integration to quantify spectra for dissolved organic matter. *Environmental Science & Technology*, 2003, **37**(24): 5701–5710

40. Yu L, Bian C, Zhu N, Shen Y, Yuan H. Enhancement of methane production from anaerobic digestion of waste activated sludge with choline supplement. *Energy*, 2019, **173**: 1021–1029

41. Klocke M, Mähnert P, Mundt K, Souidi K, Linke B. Microbial community analysis of a biogas-producing completely stirred tank reactor fed continuously with fodder beet silage as mono-substrate. *Systematic and Applied Microbiology*, 2007, **30**(2): 139–151

42. Zhao X, Liu J, Liu J, Yang F, Zhu W, Yuan X, Hu Y, Cui Z, Wang X. Effect of ensiling and silage additives on biogas production and microbial community dynamics during anaerobic digestion of switchgrass. *Bioresource Technology*, 2017, **241**: 349–359

43. Turker G, Aydin S, Akyol C, Yenigun O, Ince O, Ince B. Changes in microbial community structures due to varying operational conditions in the anaerobic digestion of oxytetracycline-medicated cow manure. *Applied Microbiology and Biotechnology*, 2016, **100**(14): 6469–6479

44. Solli L, Havelsrud O E, Horn S J, Rike A G. A metagenomic study of the microbial communities in four parallel biogas reactors. *Biotechnology for Biofuels*, 2014, **7**(1): 146

45. Zhang Z, Gao P, Cheng J, Liu G, Zhang X, Feng Y. Enhancing anaerobic digestion and methane production of tetracycline wastewater in EGSB reactor with GAC/NZVI mediator. *Water Research*, 2018, **136**: 54–63

46. Jensen M B, de Jonge N, Dolriis M D, Kragelund C, Fischer C H, Eskesen M R, Noer K, Moller H B, Ottosen L D M, Nielsen J L, Kofoed M V W. Cellulolytic and xylanolytic microbial communities associated with lignocellulose-rich wheat straw degradation in anaerobic digestion. *Frontiers in Microbiology*, 2021, **12**: 645174

47. Yun H, Liang B, Ding Y C, Li S, Wang Z F, Khan A, Zhang P, Zhang P Y, Zhou A, Wang A, Li X. Fate of antibiotic resistance genes during temperature-changed psychrophilic anaerobic digestion of municipal sludge. *Water Research*, 2021, **194**: 116926

48. Nobu M K, Narihiro T, Kuroda K, Mei R, Liu W T. Chasing the elusive Euryarchaeota class WSA2: genomes reveal a uniquely fastidious methylreducing methanogen. *ISME Journal*, 2016, **10**(10): 2478–2487

49. Lang K, Schuldes J, Klingl A, Poehlein A, Daniel R, Brune A. New mode of energy metabolism in the seventh order of methanogens as revealed by comparative genome analysis of "*Candidatus* Methanoplasma termitum". *Applied and Environmental Microbiology*, 2015, **81**(4): 1338–1352

50. Wang Y, Ren G, Zhang T, Zou S, Mao C, Wang X. Effect of magnetite powder on anaerobic co-digestion of pig manure and wheat straw. *Waste Management*, 2017, **66**: 46–52

51. Anderson G K, Kasapgil B, Ince O. Microbiological study of two-stage anaerobic digestion during start-up. *Water Research*, 1994, **28**(11): 2383–2392

52. Wandera S M, Westerholm M, Qiao W, Yin D, Jiang M M, Dong R. The correlation of methanogenic communities' dynamics and process performance of anaerobic digestion of thermal hydrolyzed sludge at short hydraulic retention times. *Bioresource Technology*, 2019, **272**: 180–187

53. Park J G, Lee B, Park H R, Jun H B. Long-term evaluation of methane production in a bio-electrochemical anaerobic digestion reactor according to the organic loading rate. *Bioresource Technology*, 2019, **273**: 478–486

54. Wu Y Q, Song K. Anaerobic co-digestion of waste activated sludge and fish waste: methane production performance and mechanism analysis. *Journal of Cleaner Production*, 2021, **279**: 123678

55. Chen H, Rao Y, Cao L, Shi Y, Hao S, Luo G, Zhang S. Hydrothermal conversion of sewage sludge: focusing on the characterization of liquid products and their methane yields. *Chemical Engineering Journal*, 2019, **357**: 367–375

56. Lei Y Q, Sun D Z, Dang Y, Feng X L, Huo D, Liu C Q, Zheng K, Holmes D E. Metagenomic analysis reveals that activated carbon aids anaerobic digestion of raw incineration leachate by promoting direct interspecies electron transfer. *Water Research*, 2019, **161**: 570–580

57. Ziels R M, Sousa D Z, Stensel H D, Beck D A C. DNA-SIP based genome-centric metagenomics identifies key long-chain fatty acid-degrading populations in anaerobic digesters with different feeding frequencies. *ISME Journal*, 2018, **12**(1): 112–123

58. Delforno T P, Lacerda G V Jr, Sierra-Garcia I N, Okada D Y, Macedo T Z, Varesche M B A, Oliveira V M. Metagenomic analysis of the microbiome in three different bioreactor configurations applied to commercial laundry wastewater treatment. *Science of the Total Environment*, 2017, **587–588**: 389–398

59. Delforno T P, Macedo T Z, Midoux C, Lacerda G V Jr, Rué O, Mariadassou M, Loux V, Varesche M B A, Bouchez T, Bize A, Oliveira V M. Comparative metatranscriptomic analysis of anaerobic digesters treating anionic surfactant contaminated wastewater. *Science of the Total Environment*, 2019, **649**: 482–494

60. Hassa J, Maus I, Off S, Pühler A, Scherer P, Klocke M, Schlüter A. Metagenome, metatranscriptome, and metaproteome approaches unraveled compositions and functional relationships of microbial communities residing in biogas plants. *Applied Microbiology and Biotechnology*, 2018, **102**(12): 5045–5063

61. Hochheimer A, Schmitz R A, Thauer R K, Hedderich R. The

tungsten formylmethanofuran dehydrogenase from *Methanobacterium thermoautotrophicum* contains sequence motifs characteristic for enzymes containing molybdopterin dinucleotide. *European Journal of Biochemistry*, 1995, **234**(3): 910–920

62. Maus I, Wibberg D, Stantscheff R, Cibis K, Eikmeyer F G, König H, Pühler A, Schlüter A. Complete genome sequence of the hydrogenotrophic archaeon *Methanobacterium* sp Mb1 isolated from a production-scale biogas plant. *Journal of Biotechnology*, 2013, **168**(4): 734–736

63. Kitamura K, Fujita T, Akada S, Tonouchi A. *Methanobacterium kanagiense* sp nov., a hydrogenotrophic methanogen, isolated from rice-field soil. *International Journal of Systematic and Evolutionary Microbiology*, 2011, **61**(Pt 6): 1246–1252

64. Ermler U, Grabarse W, Shima S, Goubeaud M, Thauer R K. Crystal structure of methyl coenzyme M reductase: the key enzyme of biological methane formation. *Science*, 1997, **278**(5342): 1457–1462

65. Li Y, Leahy S C, Jeyanathan J, Henderson G, Cox F, Altermann E, Kelly W J, Lambie S C, Janssen P H, Rakonjac J, Attwood G T. The complete genome sequence of the methanogenic archaeon ISO4-H5 provides insights into the methylotrophic lifestyle of a ruminal representative of the Methanomassiliicoccales. *Standards in Genomic Sciences*, 2016, **11**(1): 59